Stem Cell Reports
Article

ISSCR

OPEN ACCESS

High-throughput screening on cochlear organoids identifies VEGFR-MEK-TGFB1 signaling promoting hair cell reprogramming

Qing Liu,[1] Linqing Zhang,[1] Min-Sheng Zhu,[1] and Guoqiang Wan[1,2,3,4,*]

[1]MOE Key Laboratory of Model Animal for Disease Study, Department of Otorhinolaryngology-Head and Neck Surgery, The Affiliated Drum Tower Hospital of Medical School, Model Animal Research Center of Medical School, Nanjing University, Nanjing 210032, China
[2]Research Institute of Otolaryngology, No. 321 Zhongshan Road, 210008 Nanjing, China
[3]Jiangsu Key Laboratory of Molecular Medicine, Medical School of Nanjing University, Nanjing 210032, China
[4]Institute for Brain Sciences, Nanjing University, Nanjing 210032, China
*Correspondence: guoqiangwan@nju.edu.cn
https://doi.org/10.1016/j.stemcr.2021.08.010

SUMMARY

Hair cell degeneration is a major cause of sensorineural hearing loss. Hair cells in mammalian cochlea do not spontaneously regenerate, posing a great challenge for restoration of hearing. Here, we establish a robust, high-throughput cochlear organoid platform that facilitates 3D expansion of cochlear progenitor cells and differentiation of hair cells in a temporally regulated manner. High-throughput screening of the FDA-approved drug library identified regorafenib, a VEGFR inhibitor, as a potent small molecule for hair cell differentiation. Regorafenib also promotes reprogramming and maturation of hair cells in both normal and neomycin-damaged cochlear explants. Mechanistically, inhibition of VEGFR suppresses TGFB1 expression via the MEK pathway and TGFB1 downregulation directly mediates the effect of regorafenib on hair cell reprogramming. Our study not only demonstrates the power of a cochlear organoid platform in high-throughput analyses of hair cell physiology but also highlights VEGFR-MEK-TGFB1 signaling crosstalk as a potential target for hair cell regeneration and hearing restoration.

INTRODUCTION

Hearing loss is the most common sensory defect that affects more than 320 million people worldwide (Olusanya et al., 2014). Degeneration of the cochlear sensory hair cells is the primary cause of sensorineural hearing loss, which may arise from genetic defects, noise exposure, aging, ototoxicity, and other environmental insults (Wang and Puel, 2018). Upon ototoxic or noise damage, birds and amphibians can regenerate the lost hair cells either by direct trans-differentiation or asymmetric division of the surrounding supporting cells (Warchol, 2011). However, in the postnatal mammalian cochlea, although multiple cochlear supporting cells exist, these cells are post-mitotic and do not regenerate hair cells, thus leading to permanent hearing loss when hair cells are damaged (Rubel et al., 2013).

Attempts have been made to induce proliferation and differentiation of the otherwise quiescent mammalian supporting cells, among which the LGR5+ supporting cells are the most attractive candidates (Jansson et al., 2015). LGR5 is a WNT co-receptor and a well-recognized progenitor cell marker in multiple tissues, including intestine, liver, and skin (Barker et al., 2013). WNT activation of the LGR5+ supporting cells leads to spontaneous hair cell conversion in neonatal cochlea (Bramhall et al., 2014; Samarajeewa et al., 2019), which can be further promoted by induction of ATOH1 (Kuo et al., 2015), reduction of SOX2 (Atkinson et al., 2018), or inhibition of NOTCH (Bramhall et al., 2014). However, functional recovery remains a significant challenge, as either the induced hair cells are immature and die eventually or the hair cell induction fails to occur beyond 1 week of age (Samarajeewa et al., 2019). Although NOTCH inhibition has been shown to promote functional hair cell trans-differentiation in adult *in vivo*, the efficiency remains low and hair cells are regenerated at the expense of supporting cells (Mizutari et al., 2013). Therefore, additional signals and pathways required for efficient hair cell differentiation, maturation, and survival remain to be identified.

Large-scale screening to identify modulators for hair cell toxicity, protection, or regeneration has been largely carried out with zebrafish lateral line models (Coffin et al., 2010) or cochlear HEI-OC1 cells (Teitz et al., 2018). However, unlike mammalian hair cells, zebrafish hair cells can spontaneously regenerate (Warchol, 2011) and the cultured HEI-OC1 cells do not fully recapitulate the structural and functional characteristics of native hair cells (Kalinec et al., 2003). Thus, the relevance of these models for studying mammalian hair cell differentiation is limited. Recent developments and applications of tissue organoids have provided unprecedented opportunities for disease modeling, omics profiling, and high-throughput screening studies (Fatehullah et al., 2016). Inner ear organoids from pluripotent stem cells or cochlear organoids from neonatal mouse cochlear progenitors have also been developed in recent years (Koehler et al., 2013, 2017; McLean et al., 2017). These organoids resemble some of the key inner ear development processes and are able to differentiate into hair cells with remarkable structural and functional

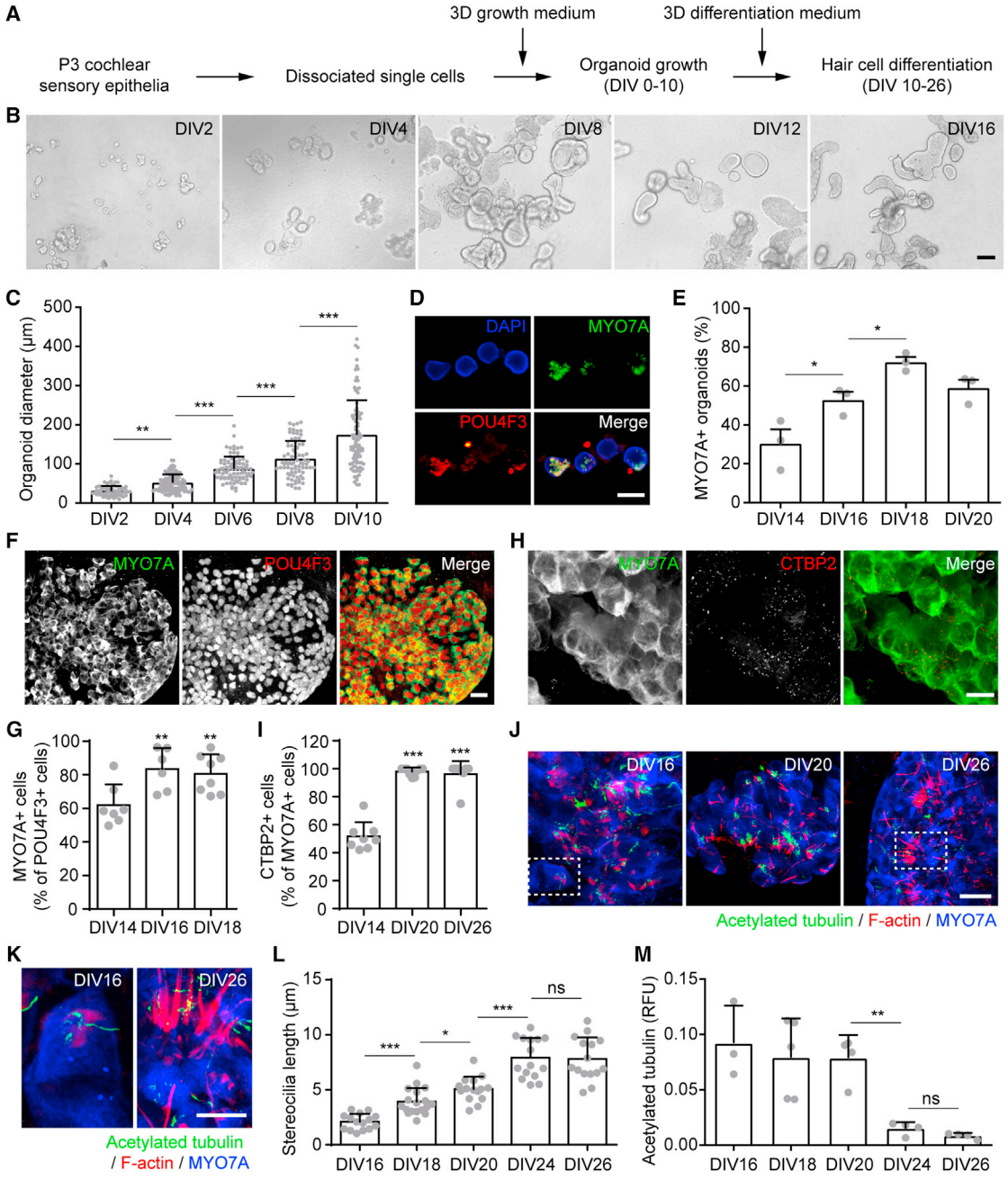

Figure 1. Highly efficient expansion and differentiation of cochlear organoids in 3D culture

(A) Experimental scheme of cochlear organoid expansion and differentiation. DIV, day *in vitro*.

(B) Bright-field images of cochlear organoids at DIV2–16. Scale bar, 200 μm.

(C) Gradual increase in cochlear organoid diameters at expansion stages (DIV2–DIV10). Error bars represent mean ± SD. n = 113 (DIV2), 108 (DIV4), 127 (DIV6), 113 (DIV8), or 132 (DIV10) organoids pooled from three independent experiments. **p < 0.01, ***p < 0.001 by one-way ANOVA.

(D) Differentiated cochlear organoids (DIV18) expressed hair cell markers MYO7A (green) and POU4F3 (red). Scale bar, 500 μm.

(E) Increase in percentage of organoids expressing hair cell marker MYO7A at DIV14, DIV16, and DIV18. Error bars represent mean ± SEM. n = 3 independent experiments with 150–250 organoids at each condition. *p < 0.05 by one-way ANOVA.

(legend continued on next page)

similarities to the native hair cells (Liu et al., 2016; Roccio and Edge, 2019; Schaefer et al., 2018).

Here, we establish a high-throughput screening platform using cochlear organoids robustly expanded from neonatal mice. Using a new hair cell-specific reporter mouse, we screened the FDA-approved drug library and identified a small-molecule, regorafenib, promoting hair cell reprogramming in a NOTCH-independent, VEGFR-MEK-TGFB1 axis-dependent signaling pathway.

RESULTS

Cochlear organoids can be expanded and differentiated into hair cells at high efficiency in 3D culture

Progenitor cells from neonatal cochlea can be expanded and differentiated into hair cell-like cells in 3D culture as cochlear organoids (Lenz et al., 2019; McLean et al., 2017; Roccio and Edge, 2019). To examine the efficiency of progenitor cell expansion and hair cell differentiation, cochlear sensory epithelial cells from postantal day 3 (P3) mouse were dissociated and subjected to a stepwise culture protocol for expansion and differentiation (Figure 1A). Cochlear organoids showed gradual increase in sizes during the expansion stage (DIV0-10; Figures 1B and 1C). Replacement of the expansion medium with differentiation medium at DIV10 onward induced expression of hair cell markers, including POU4F3 and MYO7A (Figure 1D). Expression of MYO7A was first observed at 4 days post-differentiation (DIV14), and more than 60% of the organoids contained MYO7A+ hair cells by DIV18 (Figure 1E). The differentiated organoids also expressed other mature inner hair cell markers, including PVALB (Figure S1A), CALB2 (Figure S1B), and OTOF (Figure S1C). We have attempted to immuno-stain the mature OHC marker SLC26A5, but did not observe reliable signals from the differentiated hair cells.

To examine the dynamics in maturation of the induced hair cells, we further analyzed the temporal changes in hair cell markers and structures of the differentiating cochlear organoids. qPCR analysis of the differentiating organoids (DIV10–DIV20) showed time-dependent increases in expression levels of multiple hair cell-specific genes, including *Atoh1*, *Pou4f3*, *Myo7a*, *Gfi1*, *Tmc1*, *Slc17a8*, *Chrna9*, and *Cacna1d* (Figure S1D). The total mRNA levels of *Sox2* did not show significant alteration in cochlear organoids (Figure S1D; *Sox2*). Both POU4F3 and MYO7A are well-known hair cell markers; however, POU4F3 was first detected in embryonic day 13 (E13) mouse cochlear hair cells (Xiang et al., 2003), while MYO7A expression is only observed as late as E15.5 (Chen et al., 2002). Correspondingly, in cochlear organoids at DIV14, only 60% of the POU4F3+ hair cells co-expressed MYO7A (Figure 1G). The ratio of POU4F3 and MYO7A co-expression significantly increased to more than 80% at DIV16 and DIV18 (Figures 1F and 1G), consistent with their expression patterns during embryonic development. The synaptic ribbon is a structural hallmark of functional hair cells, which tethers presynaptic vesicles at afferent synapses (Fuchs et al., 2003) and can be labeled by ribbon-specific marker RIBEYE/CTBP2 (Schmitz et al., 2000). While only about 50% of the MYO7A+ cells showed CTBP2 labeling at DIV14, almost all induced hair cells expressed CTBP2+ ribbon puncta at DIV20 and DIV26 (Figures 1H and 1I). Hair cell stereocilia, which are essential for hair cell mechanotransduction (Fettiplace and Hackney, 2006), also showed gradual elongation during organoid differentiation (Figures 1J–1L). Importantly, the kinocilia, developmental structures present in immature but not mature cochlear hair cells (Liu et al., 2018b), were gradually lost by DIV24 and DIV26 (Figures 1J, 1K, and 1M). These findings indicate that expansion and differentiation of the cochlear organoids is highly efficient, and hair cells differentiated within the organoids show developmental maturation.

Cochlear organoids are derived from both LGR5+ and LGR5– progenitor cells

The cochlear sensory epithelium consists of hair cells and multiple subtypes of SOX2+ non-sensory supporting cells

(F and G) Increase in percentage of POU4F3+ cells co-expressing MYO7A in cochlear organoids at DIV14, DIV16, and DIV18. (F) Confocal images (DIV18) and (G) percentage of organoids co-expressing POU4F3 and MYO7A. Scale bar, 20 μm. Error bars represent mean ± SEM. n = 6–8 wells with 100–200 organoids at each condition. **p < 0.01 by one-way ANOVA.

(H and I) Increase in percentage of MYO7A+ cells expressing CTBP2+ ribbon puncta in cochlear organoids at DIV14, DIV20, and DIV26. (H) Confocal images (DIV20) and (I) percentage of CTBP2+ hair cells. Scale bar, 10 μm. Error bars represent mean ± SEM. n = 6–8 wells with 100–200 organoids at each condition. ***p < 0.001 by one-way ANOVA.

(J and K) Gradual maturation of ciliary morphology in organoids at DIV16, DIV20, and DIV26. (J) F-Actin (red) and acetylated tubulin (green) show the stereocilia and kinocilia, respectively. (K) Magnified views of dotted areas shown in (J). Scale bars, 10 μm (J) and 5 μm (K).

(L) Gradual increase of stereocilia length of hair cells in DIV16–DIV26 organoids. Error bars represent mean ± SEM. n = 15–18 images with 50–100 organoids at each condition. *p < 0.05 and ***p < 0.001 by one-way ANOVA.

(M) Reduced relative immunofluorescent intensity of acetylated tubulin in DIV16–DIV26 organoids. Error bars represent mean ± SEM. n = 3 independent experiments with 50–100 organoids at each condition. **p < 0.01 by one-way ANOVA.

See also Figure S1.

(Wan et al., 2013). Previous reports indicate that the LGR5+ supporting cells, which include greater epithelial ridge, inner border, inner pillar, and the third row of Deiters cells, are resident cochlear progenitors that undergo proliferation and differentiation after NOTCH inhibition and/or WNT activation (Bramhall et al., 2014; McGovern et al., 2019; Shi et al., 2012). In addition, PLP1+ inner border and inner phalangeal cells have been shown to spontaneously regenerate in injured neonatal cochlea (Mellado Lagarde et al., 2014); however, whether these cells can be expanded and reprogrammed to hair cells remains unknown. To examine the contributions of the supporting cell subtypes to cochlear organoid growth and differentiation, we performed lineage-tracing experiments using cochlear cells of P3 pups born to *Rosa26*-ACTB-*mTmG* mice mated with different Cre lines. In brief, single cells from P3 sensory epithelia of *Lgr5-CreER*:*mTmG*, *Sox2-CreER*:*mTmG*, or *Plp1-CreER*:*mTmG* mice (Figure 2A) were isolated and subjected to organoid culture in the presence of 4-OH tamoxifen. After induced hair cell differentiation, the proportion of lineage-traced (Cre+ or mG+) or untraced (Cre– or mG–) organoids and MYO7A+ or MYO7A– organoids was analyzed.

Robust recombination and mGFP labeling were observed in cochlear organoids lineage traced with *Lgr5-CreER*, *Sox2-CreER*, and *Plp1-CreER* (Figures 2B–2E). At DIV18, we found that more than 90% and about 80% of the cochlear organoids were derived from SOX2+ cells and LGR5+ cells, respectively, whereas PLP1+ cells contributed to only about 20% of the total organoids (Figure 2F; Cre+). Interestingly, although MYO7A+ cells were all derived from SOX2+ cell lineage, not all SOX2+ cells could differentiate into MYO7A+ cells (Figures 2C and 2F), suggesting that some of the supporting cells retained proliferative capacity but were unable to differentiate into MYO7A+ cells at current experimental conditions. In contrast, albeit at a smaller proportion (~20%), almost all the PLP1+ organoids were successfully differentiated into MYO7A+ cells (Figures 2D and 2F), highlighting the potency of inner border and inner phalangeal cells as hair cell progenitors. Similar to SOX2+ organoids, not all LGR5+ organoids could differentiate into MYO7A+ cells (Figures 2E and 2F). This is consistent with a previous report that only a subset of LGR5+ cells can be converted to hair cell-like cells when forced to overexpress ATOH1 and a constitutively active form of β-catenin (Kuo et al., 2015). Intriguingly, hair cell differentiation was observed in a small population of LGR5– (and presumably SOX2+) cells (Figure 2F). These MYO7A+/LGR5– organoids showed a gradual increase in proportion from DIV16 to DIV20 (Figure 2G), indicating that a subpopulation of LGR5– cells may also serve as progenitors that can be differentiated into hair cell at a slower kinetics than LGR5+ cells. In summary, our study demonstrates that both LGR5+ and LGR5– cells contributed to expansion and hair cell differentiation of cochlear organoids.

Culture optimization and further expansion of cochlear organoids

To increase the yield of cochlear organoids for high-throughput experiments, we optimized the culture conditions for passaging and further expansion (Figure S2A). While initial culture conditions using 50 ng/mL EGF and 3 μM CHIR99021 supported growth of the first-passage organoids, these conditions failed to maintain organoid growth after further dissociation and passaging. We performed concentration gradients of EGF and CHIR99021, two major determinants of organoid growth based on our initial screening, to identify the optimal condition for passage 2 organoid expansion. We found that, for passage 2 organoids, a reduced concentration of CHIR99021 (2 μM) was required (Figure S2B). Furthermore, a reduced concentration of EGF (25 ng/mL) was optimal for organoid expansion (Figure S2C).

We then characterized the growth and differentiation of passage 2 cochlear organoids under the optimized culture conditions (Figure S2D). Growth of passage 2 cochlear organoids was demonstrated by gradual increase in diameter from DIV10 to DIV16, but their overall sizes were significantly smaller than passage 1 organoids (Figures S2E and S2F). Despite their smaller sizes, the relative compositions of LGR5+ organoids (Figures S2G and S2H) and the ability to support hair cell differentiation (Figures S2I and S2J) were indistinguishable between passage 1 and passage 2 organoids. As a result, the culture and expansion of passage 2 organoids allowed approximately 400-fold increase in number of organoids compared with passage 1, and allowed a total of 6,000-fold increase in sample throughput, i.e., 6,000 organoids derived from a single cochlear sensory epithelium.

FDA-approved small-molecule screening of cochlear organoids identifies Regorafenib in promoting hair cell differentiation

We recently established a novel hair cell fate reporter mouse model by knocking in EGFP-IRES-CreER into the *Pou4f3* locus, which allowed hair cell-specific EGFP and CreER expression driven by the endogenous *Pou4f3* promoter (Du et al., 2020; Zhu et al., 2020). In the heterozygous *Pou4f3(EGFP/+)* mice, EGFP expression was specifically and robustly detected in hair cells of P0 (Figure S3A) and P28 (Figure S3B) cochlea, as well as in P0 and P28 utricular hair cells (Figures S3C and S3D). These *Pou4f3(EGFP/+)* knockin mice did not display auditory dysfunction until at least 3 months age (Zhu et al., 2020) and were suitable for studying hair cell development and lineage specification.

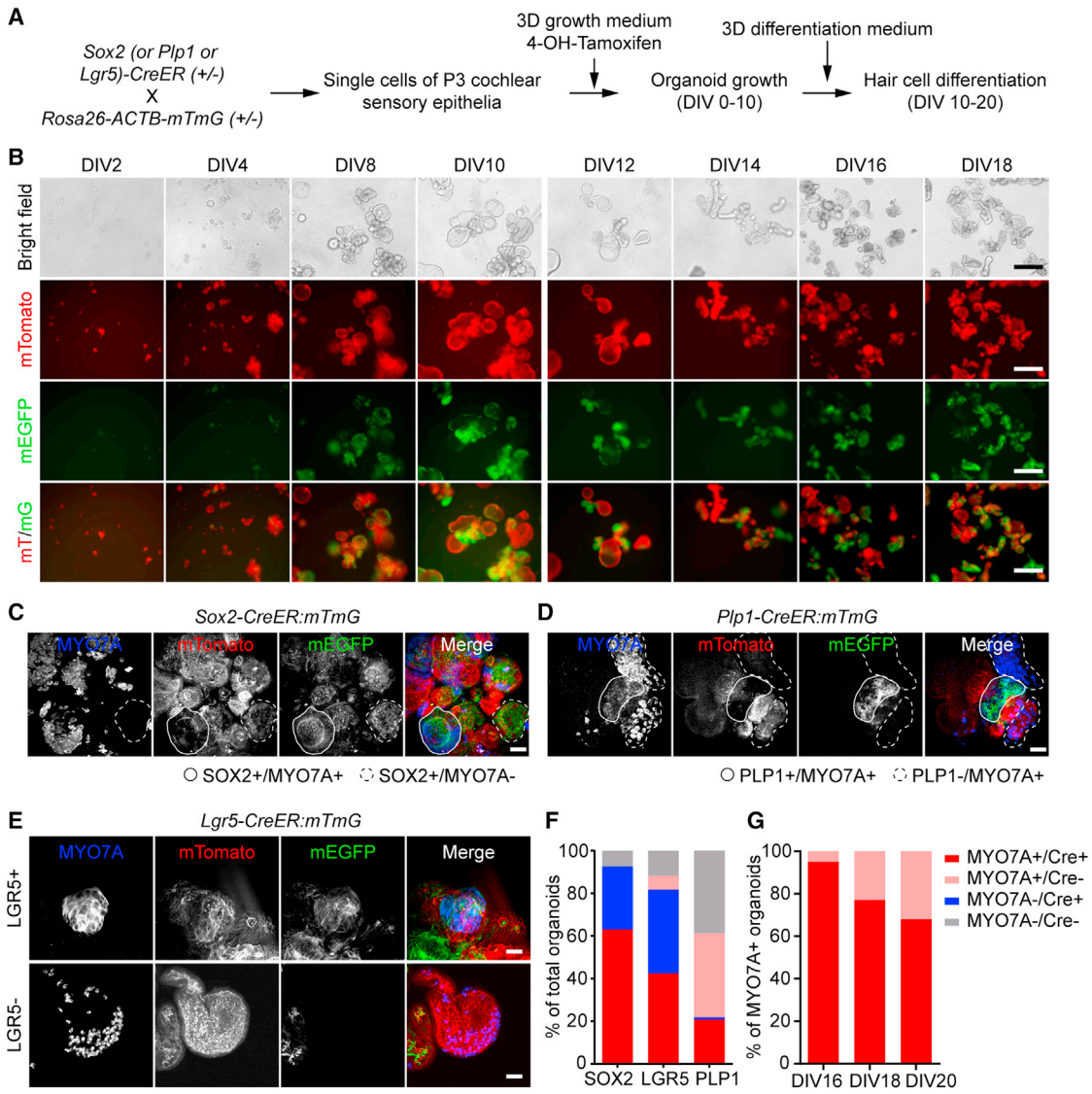

Figure 2. Cochlear organoids are predominantly derived from LGR5+ progenitor cells

(A) Experiment scheme of organoid lineage tracing using *Sox2-CreER*, *Plp1-CreER*, or *Lgr5-EGFP-IRES-CreER* (*Lgr5-CreER*) mice.

(B) Bright-field and fluorescent images of cochlear organoids at expansion (DIV2–DIV10) and differentiation (DIV12–DIV18) stages. mEGFP fluorescence indicates lineage-traced organoids using *Lgr5-CreER*. Scale bars, 500 μm.

(C) Most MYO7A+ organoids were derived from SOX2+ progenitor cells. Scale bar, 50 μm.

(D) Organoids derived from PLP1+ progenitor cells were in small numbers but effectively differentiate into MYO7A+ organoids. Scale bar, 50 μm.

(E) Both LGR5+ and LGR5– organoids differentiated into hair cells. Confocal images of DIV18 organoids immunostained by MYO7A. Scale bars, 50 μm.

(F) Proportions of MYO7A+ and MYO7A– organoids (DIV18) lineage traced with *Sox2-CreER*, *Lgr5-CreER*, or *Plp1-CreER*. All ratios were calculated from 50 to 150 organoids of each condition from two independent lineage-tracing experiments.

(G) Proportions of MYO7A+ organoids lineage traced with (dark red) or without (light red) *Lgr5-CreER*. All ratios were calculated from 50 to 150 organoids of each condition from two independent lineage-tracing experiments.

A previous report showed that WNT activation and γ-secretase/NOTCH inhibition synergistically promotes hair cell differentiation in cochlear organoids (McLean et al., 2017). We found that γ-secretase inhibition by LY411575 was sufficient for efficient hair cell conversion (Figures S3E and S3G); while WNT activation by CHIR99021 was critical for the survival of cochlear organoids differentiated by LY411575 (Figures S3E and S3F). Therefore, to discover

novel signals that promote hair cell differentiation, we screened 1,004 Food and Drug Administration (FDA)-approved small molecules in differentiating cochlear organoids in the presence of CHIR99021 and the absence of LY411575 (Figure 3A; Data S1, sheets 1 and 2). For this purpose, we used passage 2 cochlear organoids derived from the *Pou4f3(EGFP/+)* mice, in which the differentiated hair cells could be faithfully labeled by the expression of *Pou4f3*-driven EGFP (Figures 3B and 3C).

High-throughput screening of the small molecules identified 91 candidates that promoted hair cell differentiation according to the selection criteria (Figure 3C; Data S1, sheet 3). Among the candidate small molecules, regorafenib was found to reproducibly promote hair cell differentiation at concentrations of 2, 5, and 10 μM (Figure 3E). A higher dose of regorafenib (15 μM) appeared to be toxic to the differentiating organoids (Figure 3E). Importantly, regorafenib at 5 μM exhibited comparable potency in hair cell induction as the positive control LY411575 (Figure 3E). In addition, as with LY411575, regorafenib treatment also promoted the formation of presynaptic ribbons in the induced hair cells (Figures 3F–3H). Thus, our study established a high-throughput cochlear organoid screening platform and identified a novel small-molecule candidate, regorafenib, for promoting hair cell differentiation and developmental maturation.

Regorafenib promotes hair cell reprogramming in cochlear explants by inhibiting VEGFR

To validate the effect of regorafenib on cochlear tissues, we cultured P3 cochlear explants (Figure 4A) and treated them with vehicle, CHIR99021 alone or with γ-secretase inhibitor DAPT or regorafenib over the course of 5 days. Interestingly, CHIR99021 alone promoted hair cell differentiation only in the apical turns of the cochlear explants (Figure 4B), which was not potentiated by either DAPT or regorafenib. However, both DAPT and regorafenib were able to synergize with CHIR99021 to promote hair cell differentiation at the middle and basal cochlear turns (Figure 4B). Regorafenib promoted hair cell differentiation in a dose-dependent manner from 0.5 to 1.5 μM (Figures 4B and 4C) at the middle turn. The effective concentrations of regorafenib on the cochlear explants were lower than that on the organoids (Figure 3E), which is likely due to better accessibility of the small molecules to the supporting cells of cochlear explants compared with the organoids. As the integrity of hair cell morphology and effects of hair cell differentiation were most consistent at middle turns, we only examined the cochlear middle turns in subsequent experiments.

Interestingly, regorafenib treatment alone failed to promote an increase in hair cell counts, similar to CHIR99021 treatment alone in the middle turns (Figure 4D). These results suggested that the effects of regorafenib were dependent on the activation of WNT signaling. Co-immunostaining of hair cell markers (MYO7A and POU4F3) with supporting cell marker SOX2 revealed that large number of induced hair cells retained SOX2 expression after CHIR99021 and regorafenib co-treatment (Figure 4E). As WNT activation was sufficient to promote supporting cell proliferation shown by increased SOX2+ cells in CHIR99021-treated explants (Figure 4F), it is likely that regorafenib promoted reprogramming of hair cells from the SOX2+ supporting cells expanded by WNT activation. To demonstrate that the induced hair cells were indeed derived from cochlear supporting cells, we performed a lineage-tracing study where the SOX2+ supporting cells were permanently traced by tdTomato after tamoxifen treatment. While the CHIR99021 treatment alone did not induce hair cell differentiation, 1 μM regorafenib co-treatment promoted trans-differentiation of tdTomato+ supporting cells to MYO7A+ hair cells (Figures 4G and 4H). These findings indicate that regorafenib, in combination with CHIR99021, promotes hair cell reprogramming from supporting cells in cochlear explants.

Regorafenib is a multi-kinase inhibitor targeting VEGFR, platelet-derived growth factor receptors (PDGFRs), RAF1, RET, KIT, and other oncogenic kinases (Grothey et al., 2013; Wilhelm et al., 2011). To probe the specific targets of regorafenib in promoting hair cell reprogramming, we evaluated the effects of other regorafenib family molecules that share common but non-overlapping kinase targets (Figure S4A). Among the six additional inhibitors, apatinib mesylate at 10 μM (Figure S4B), cabozantinib at 1 and 2 μM (Figure S4C), and pazopanib HCl at 5–15 μM (Figure S4D) significantly induced hair cell reprogramming. VEGFR and KIT were the common targets of regorafenib and these three molecules (Figure S4A). Meanwhile, KIT kinase inhibitors masitinib (Figure S4E) and imatinib mesylate (Figure S4F) failed to exert any effect. Importantly, ZM 323881, a potent and specific inhibitor for VEGFR2 without detectable effects on PDGFRs, FGFRs, EGFRs, or ERBB2, promoted hair cell reprogramming at a concentration of 50 nM (Figure S4G). Thus, we conclude that VEGFR is the most likely target of regorafenib in promoting hair cell reprogramming.

Regorafenib promotes hair cell reprogramming and maturation in neomycin-injured cochlear explants

Various insults, such as noise exposure, aging, ototoxins, and genetic defects can result in hair cell degeneration (Wagner and Shin, 2019). We next examined if regorafenib could promote hair cell regeneration in P3 cochlear tissues injured by the ototoxin neomycin (Figure 5A). CHIR99021 alone (vehicle medium) or together with DAPT or regorafenib were added 24 h after neomycin treatment. Neomycin treatment resulted in marked loss of hair cells in cochlear

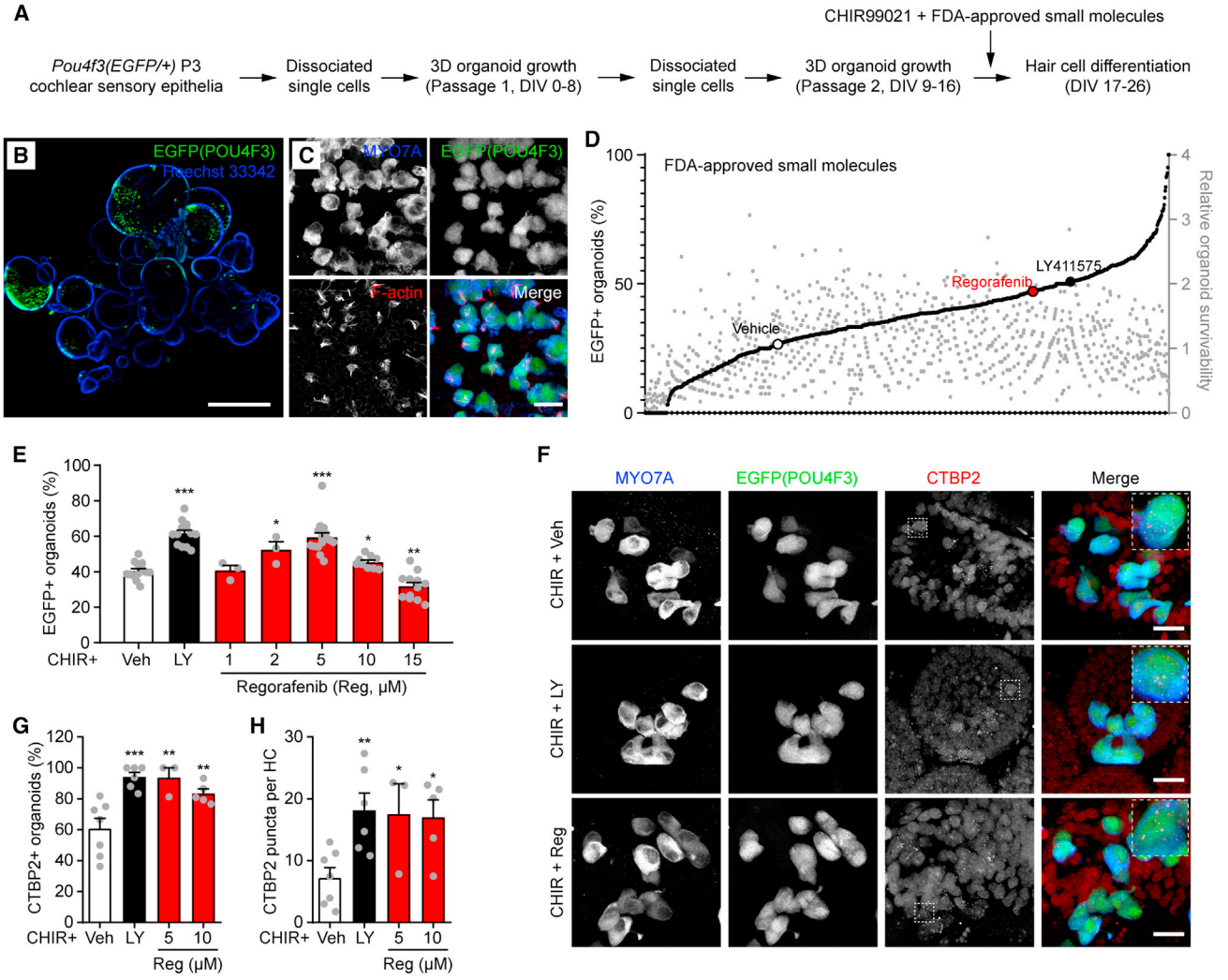

Figure 3. FDA-approved small-molecule screening of cochlear organoids identifies regorafenib in promoting hair cell differentiation

(A) Experimental scheme of small-molecule screening using *Pou4f3(EGFP/+)* reporter cochlear organoids.

(B) Representative confocal image of DIV26 *Pou4f3(EGFP/+)* reporter organoids (CHIR99021 + vehicle control) in a single well. Scale bar, 500 μm.

(C) Confocal images of EGFP+ hair cells in differentiated DIV26 *Pou4f3(EGFP/+)* reporter organoids (CHIR99021 + LY411575). Hair cells were co-labeled with MYO7A and stereocilia labeled with F-actin. Scale bar, 20 μm.

(D) Regorafenib promoted hair cell differentiation in *Pou4f3(EGFP/+)* cochlear organoids. A total of 1,004 FDA-approved small molecules (gray dots) were screened with negative (vehicle, open circle) and positive (10 μM LY411575, filled circle) controls, all in the presence of CHIR99021 (CHIR). Regorafenib is highlighted as a red circle. The left y axis shows the percentage of EGFP+ (hair cell-containing) organoids; the right y axis shows relative survivability of small-molecule-treated organoids.

(E) Dose-response of regorafenib in promoting hair cell differentiation in cochlear organoids. V, vehicle; LY, LY411575 (10 μM). Error bars represent mean ± SEM. n = 3–13 wells with 100–400 organoids at each condition. *p < 0.05, **p < 0.01, ***p < 0.001 by one-way ANOVA.

(F–H) Regorafenib promoted expression of CTBP2 in hair cells of differentiated organoids. (F) Confocal images of MYO7A (blue), EGFP(Pou4f3) (green) and CTBP2 (red) in organoids treated with vehicle, LY411575 (10 μM) or regorafenib (5 μM). Scale bar, 20 μm. Dotted small inserts represented magnified views of single hair cells with synaptic ribbons. (G) Percentage of CTBP2+ organoids and (H) numbers of CTBP2 puncta per hair cell in organoids treated with vehicle, LY411575 or regorafenib. V, vehicle; LY, LY411575 (10 μM); Reg, regorafenib.

Error bars represent mean ± SEM. n = 3–7 wells with 100–250 organoids at each condition. *p < 0.05, **p < 0.01, ***p < 0.001 by one-way ANOVA. See also Figures S2 and S3 and Data S1.

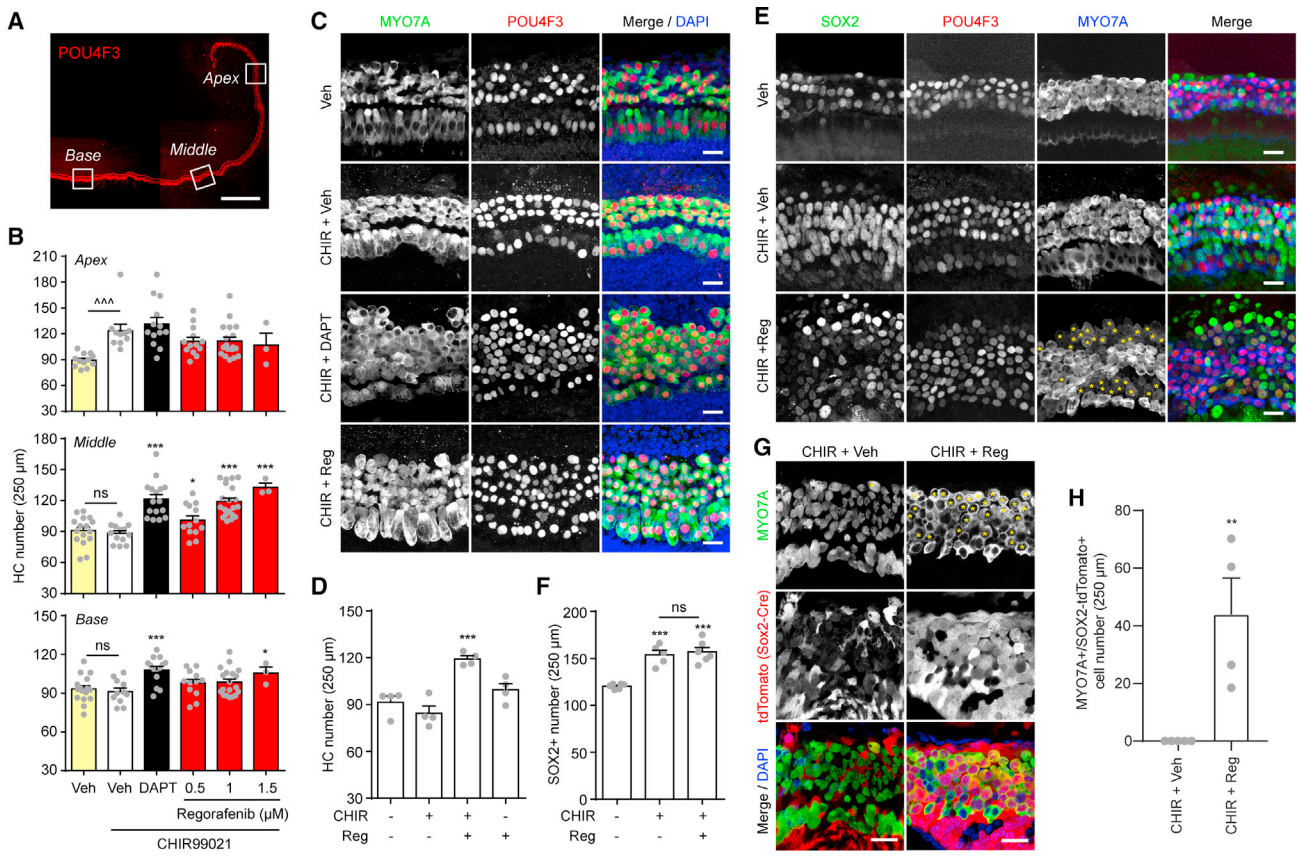

Figure 4. Regorafenib promotes hair cell reprogramming in cochlear explants

(A) Representative image of a P3 wholemount cochlear explant. Hair cells were immunostained with POU4F3 and counted at apical, middle and basal turns as depicted. Scar bar, 500 μm.

(B) Hair cell counts of cochlear explants treated with DAPT or regorafenib at apical, middle and basal turns. Error bars represent mean ± SEM. n = 12 (Veh); or 10 (CHIR + Veh); or 13 (CHIR + DAPT); or 13 (CHIR + Reg 0.5 μM); or 18 (CHIR + Reg 1 μM); or 3 (CHIR + Reg 1.5 μM) cochlear explants. *p < 0.05, ***p < 0.001 by one-way ANOVA to CHIR + Veh control; ^^^ p < 0.001 between Veh and CHIR + Veh.

(C) Confocal images of middle-turn cochlear explants immunostained with MYO7A (green) and POU4F3 (red) after treatment with vehicle, DAPT (10 μM) or regorafenib (1 μM) for 5 days. Scale bars, 20 μm.

(D) Regorafenib alone did not increase hair cell counts. Error bars represent mean ± SEM. n = 4 cochlear explants at each condition. ***p < 0.001 by one-way ANOVA.

(E) Co-immunostaining of SOX2 with hair cell markers (MYO7A and POU4F3) in cochlear explants treated with CHIR + Reg. Yellow asterisks indicate co-labeled cells. Scale bars, 20 μm.

(F) Expansion of SOX2+ supporting cells in cochlear explants treated with CHIR99021. Error bars represent mean ± SEM. n = 5–6 cochlear explants at each condition. ***p < 0.001 by one-way ANOVA.

(G) Regorafenib promoted hair cell reprogramming from SOX2+ supporting cells in cochlear explant lineages traced by *Sox2-CreER*. Yellow asterisks indicate co-labeled cells. Scale bars, 20 μm.

(H) Number of hair cells reprogrammed from SOX2-lineage-traced supporting cells. Error bars represent mean ± SEM. n = 4–5 cochlear explants at each condition. **p < 0.01 by unpaired Student's t test.

See also Figure S4.

explants cultured with vehicle medium (Figures 5B and 5C). Remarkably, both DAPT and regorafenib significantly promoted hair cell replenishment at comparable levels (Figures 5B and 5C). Lineage tracing of SOX2+ supporting cells indicate that CHIR99021 alone (vehicle medium) failed to induce hair cell reprogramming, whereas both DAPT and regorafenib promoted conversion of SOX2+ supporting cells to hair cells (Figures 5D and 5E).

To examine if DAPT and regorafenib present synergistic effects on hair cell reprogramming, we co-treated both the normal and injured P3 cochlear explants at lower doses of DAPT and regorafenib in the presence of

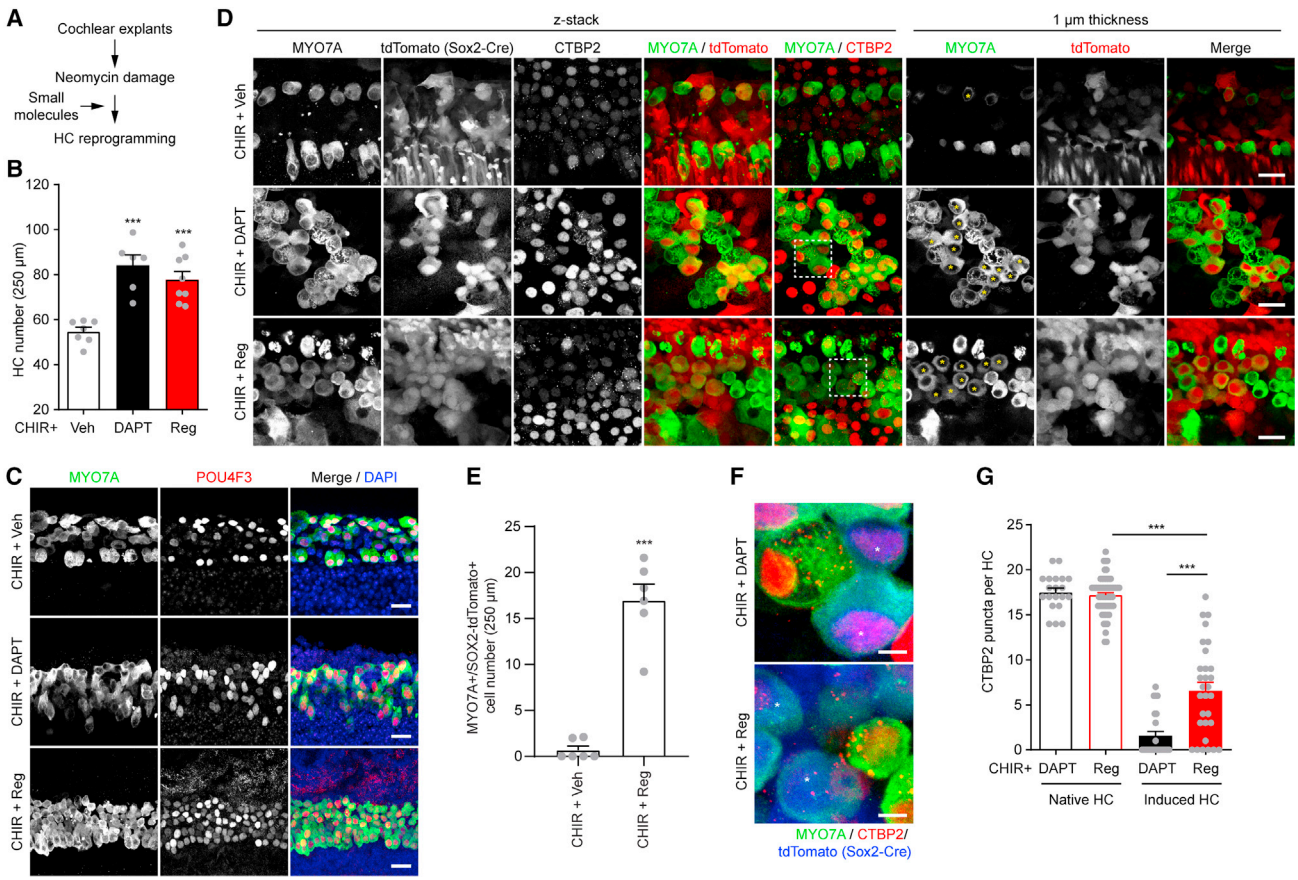

Figure 5. Regorafenib promotes hair cell reprogramming and maturation in injured cochlear explants.

(A) Flow chart of a neomycin damage experiment.

(B and C) DAPT and regorafenib promoted hair cell reprogramming in neomycin-damaged cochlear explants. (B) Hair cell counts and (C) confocal images of neomycin-damaged cochlear explants co-treated with vehicle, DAPT (10 μM), or regorafenib (1 μM) in the presence of CHIR. Surviving and reprogrammed hair cells were immunolabeled with MYO7A (green) and POU4F3 (red). Scale bars, 20 μm. Error bars represent mean ± SEM. n = 6–8 cochlear explants at each condition. ***p < 0.001 by one-way ANOVA.

(D) DAPT and regorafenib promoted hair cell reprogramming from SOX2+ supporting cells in neomycin-damaged cochlear explants lineage traced by *Sox2-CreER*. Reprogrammed hair cells were co-labeled with MYO7A and tdTomato (*Sox2-CreER*). Yellow asterisks indicate co-labeled cells. Scale bars, 20 μm.

(E) Number of hair cells reprogrammed from SOX2-lineage-traced supporting cells. Error bars represent mean ± SEM. n = 6 cochlear explants at each condition. ***p < 0.001 by Student's t test.

(F and G) Regorafenib but not DAPT promoted CTBP2 expression in reprogrammed hair cells in neomycin-damaged cochlear explants.

(F) Magnified views of the dotted area in (D) showing CTBP2 labels in hair cells reprogrammed by regorafenib but not DAPT. Asterisks indicate MYO7A+/tdTomato+ reprogrammed hair cells while the native hair cells were labeled with MYO7A but not tdTomato. Scale bars, 5 μm.

(G) Average number of CTBP2 puncta in native or induced hair cells after co-treatment with neomycin and DAPT or regorafenib. Error bars represent mean ± SEM. n = 20–60 hair cells from three cochlear explants at each condition. ***p < 0.001 by one-way ANOVA.

See also Figure S5.

CHIR99021 (Figures S5A–S5D). Lower doses of DAPT (5 μM) and regorafenib (0.5 μM) showed variable effects in promoting hair cell differentiation in both normal and injured cochlear explants. However, co-treatment of low doses of DAPT and regorafenib significantly increased hair cell density compared with either treatment alone (Figures S5A–S5D), suggesting that DAPT and regorafenib act synergistically on hair cell differentiation.

As both the γ-secretase inhibitor and regorafenib promoted expression of CTBP2 in hair cells of the cochlear organoids (Figure 3), we examined if the reprogrammed hair cells in P3 cochlear explants also displayed presynaptic ribbons. Although DAPT effectively promoted hair cell

reprogramming, most of the induced hair cells were devoid of CTBP2+ ribbon puncta (Figures 5D, 5F, and 5G). Intriguingly, hair cells induced by regorafenib showed significantly more ribbon puncta than DAPT treatment, although the ribbon density was still smaller than that of the native hair cells (Figures 5F and 5G). Therefore, our results indicate that regorafenib could mediate hair cell reprogramming and maturation in injured cochlear tissues.

Regorafenib regulates TGFB signaling pathways via MEK-dependent *Tgfb1* expression

Differential effects of DAPT and regorafenib on synaptic ribbons in induced hair cells (Figures 5F and 5G) and their synergistic effects on hair cell reprogramming (Figures S5A–S5D) implicated that these two molecules may regulate distinct signaling pathways. To address this question, we performed bulk RNA sequencing (RNA-seq) analyses on P3 cochlear explants treated 1 day with CHIR99021 alone or in combination with DAPT or regorafenib (GEO accession no. GSE139485). CHIR + DAPT only differentially regulated 31 gene products (Figure S6A; Table S1). As we would expect, biological processes involved in NOTCH signaling were ranked among the top gene ontology processes after CHIR + DAPT treatment (Figure 6A; Table S1). Heatmap analyses of the 31 genes from all three experimental conditions (CHIR + Veh, CHIR + DAPT, and CHIR + Reg) demonstrate little overlap between DAPT and regorafenib (Figure S6A). Regulation of NOTCH signaling targets and ligands including *Hey1*, *Hes1*, *Hes5*, *Jag1*, *Dll1*, and *Dll3* by DAPT at 1 and 5 days was further validated by qRT-PCR (Figure 6B). Similar to the heatmap analyses, regorafenib treatment did not affect the expression of genes involved in NOTCH signaling (Figure 6B), suggesting that regorafenib promoted hair cell reprogramming and maturation through a NOTCH-independent mechanism.

RNA-seq analyses of CHIR + regorafenib-treated P3 cochlear explants indicated that multiple pathways involving angiogenesis, chemotaxis, and inflammation were specifically regulated (Figure 6C; Table S2), consistent with the known roles of VEGFR signaling in these processes (Ferrara et al., 2003). RNA-seq heatmap analyses also showed downregulation of genes involved in angiogenesis and vascular development in CHIR + Reg samples compared with CHIR + Veh controls (Figure S6B). Downregulation of selected angiogenic and vascular genes by regorafenib but not DAPT were further validated by qRT-PCR analyses, demonstrating the expected effects of regorafenib in VEGFR signaling (Figure S6C).

Interestingly, we noticed that genes involved in cellular response to the transforming growth factor beta (TGFB) stimulus were also regulated by regorafenib (Figure 6C). qRT-PCR validation of the listed target genes (*Tgfbi*, *Fshb*, *Cdh5*, *Cx3cr1*, *Nos3*, and *Clec3b*) showed that regorafenib but not DAPT regulated TGFB signaling (Figure 6D), a process also important for cell fate determination and reprogramming (Mullen and Wrana, 2017; Yu and Feng, 2019).

We then identified that expression of the TGFB ligand *Tgfb1* was downregulated by regorafenib treatment, based on both RNA-seq and qRT-PCR analyses (Figure 7A; Table S2). It is possible that VEGFR signaling promotes expression of *Tgfb1*, which then activates TGFB signaling to suppress hair cell reprogramming. As MEK and PI3K are two key kinases downstream of VEGFR signaling (Cross et al., 2003), we next examined whether these kinases were involved in regulation of *Tgfb1* expression by VEGFR signaling in P3 cochlear explants. Co-treatment of the MEK inhibitor U0126 inhibited the effect of regorafenib on downregulation of *Tgfb1* expression in a dose-dependent manner, whereas the co-treatment of PI3K inhibitor wortmannin had no such effect (Figure 7B). Importantly, phospho-SMAD2, the downstream effector of TGFB signaling, was significantly downregulated by regorafenib treatment (Figures 7C and 7D). Together, these data indicate that the VEGFR inhibitor regorafenib did not affect NOTCH signaling but suppressed TGFB signaling by MEK-dependent downregulation of *Tgfb1* expression.

TGFB signaling mediates hair cell reprogramming by regorafenib

We next hypothesized that downregulation of *Tgfb1* expression and suppression of TGFB signaling by regorafenib contributes to hair cell reprogramming. To test this hypothesis, we co-treated the P3 cochlear explants with CHIR99021 and the TGFB receptor (TGFBR) inhibitor SB431542. As expected, SB431542 treatment inhibited both baseline and TGFB1-induced SMAD2 phosphorylation (Figure 7E). Explants with SB431542 co-treatments showed significantly more hair cells compared with CHIR99021 treatment alone (vehicle), demonstrating that direct inhibition of TGFBR also effectively promoted hair cell reprogramming (Figures 7F and 7G). However, the effects of SB431542 were less prominent than regorafenib or DAPT (Figures 7F, S5E, and S5F), which may suggest that either SB431542 was insufficient to completely inhibit TGFBR signaling or that other yet to be identified signaling pathways may have contributed to the effects of regorafenib. Consistently, co-treatment of regorafenib with SB431542 resembled the effects of regorafenib (Figures S5E and S5F).

We next examined if the effects of regorafenib were dependent on *Tgfb1* expression by co-treatments with the recombinant TGFB1. As expected, SMAD2 phosphorylation was promoted by TGFB1 and inhibited by regorafenib (Figures 7H and 7I). However, inhibition of p-SMAD2 by regorafenib was completely abolished by TGFB1

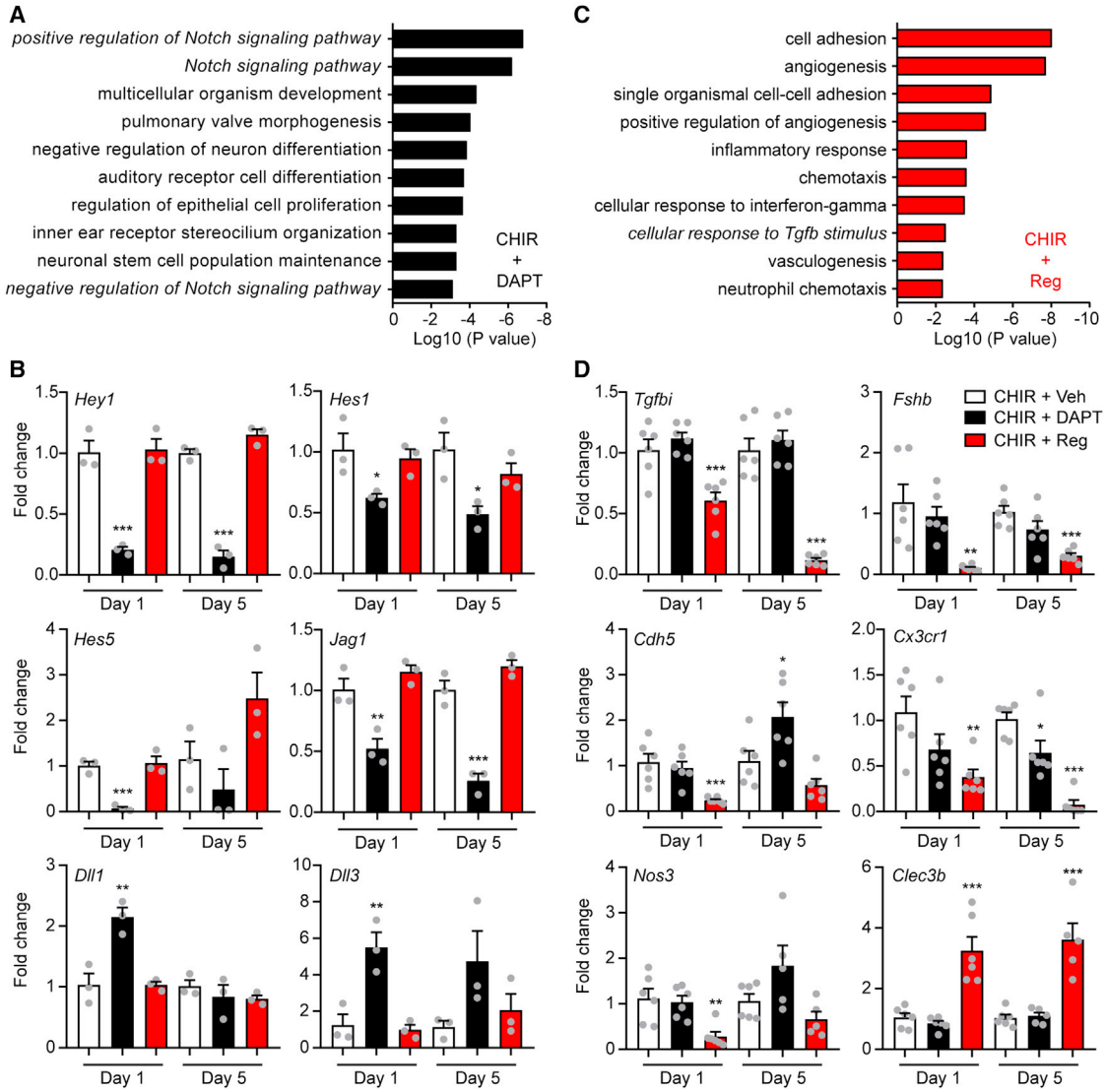

Figure 6. DAPT and regorafenib regulate distinct signaling pathways in cochlear explants

(A) NOTCH signaling pathways were enriched in the top 10 gene ontology biological processes differentially regulated by DAPT in cochlear explants.

(B) DAPT but not regorafenib regulated NOTCH pathway genes in cochlear explants treated for 1 and 5 days. Expression of NOTCH pathway genes *Hey1*, *Hes1*, *Hes5*, *Jag1*, *Dll1*, and *Dll3* were examined by qRT-PCR. Error bars represent mean ± SEM. n = 3 independent experiments with six cochlear explants at each condition. *p < 0.05, **p < 0.01, ***p < 0.001 by one-way ANOVA.

(C) TGFB signaling pathway was regulated by regorafenib in cochlear explants.

(D) Regorafenib but not DAPT regulated TGFB pathway genes in cochlear explants treated for 1 and 5 days. TGFB pathway genes *Tgfbi*, *Fshb*, *Cdh5*, *Cx3cr1*, *Nos3*, and *Clec3b* were examined by qRT-PCR. Error bars represent mean ± SEM. n = 5–6 independent experiments with 10–12 cochlear explants at each condition. *p < 0.05, **p < 0.01, ***p < 0.001 by one-way ANOVA.

See also Figure S6 and Tables S1 and S2.

co-treatment (Figures 7H and 7I). Importantly, while regorafenib promoted hair cell reprogramming, its effect was also completely abolished by co-treatment of the TGFB1 recombinant protein (Figures 7J and 7K). TGFB1 alone did not exert any effect on the hair cell density in cochlear explants (Figures 7J and 7K). A similar inhibitory effect on regorafenib-induced hair cell reprogramming was also observed with co-treatment of TGFB2 protein (Figures S5G and S5H). Thus, VEGFR-TGFB may serve as an inhibitory signal hampering hair cell reprogramming in cochlear supporting cells. Consistent with this notion, *Flt1 (Vegfr1)*, *Kdr (Vegfr2)*, *Tgfb1*, *Tgfb2*, *Tgfbr1*, and *Tgfbr2* showed

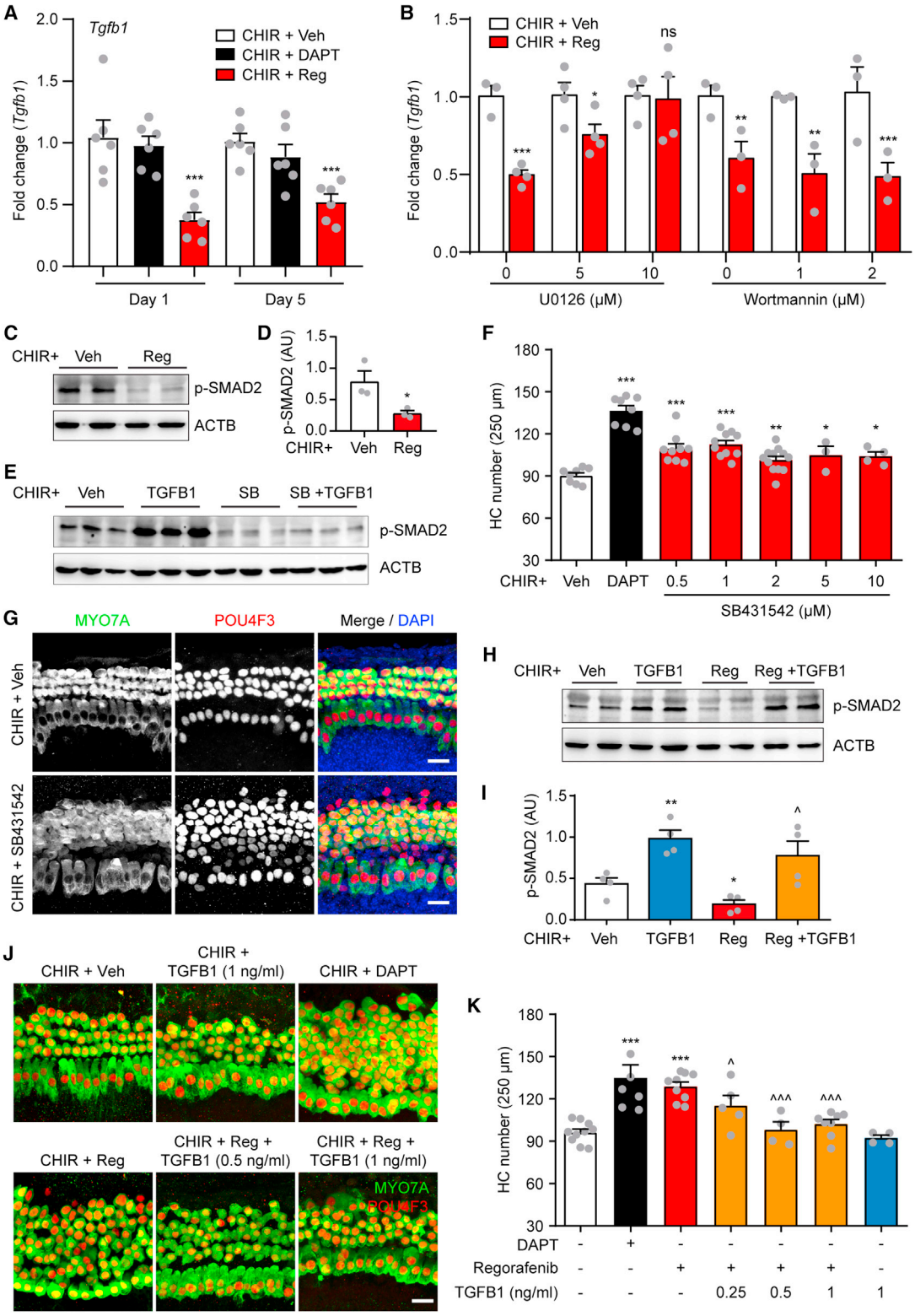

Figure 7. Regorafenib promotes hair cell reprogramming via the VEGFR-MEK-TGFB1 pathway

(A) *Tgfb1* was downregulated by regorafenib but not DAPT in cochlear explants. Error bars represent mean ± SEM. n = 6 cochlear explants from two independent experiments. ***p < 0.001 by one-way ANOVA.

(legend continued on next page)

preferential expressions in P28–P35 cochlear supporting cells (Figure S7A), according to previously published cell-type-specific RNA-seq results (Liu et al., 2018a). In addition, based on immunofluorescence data, both the VEGF receptor (KDR) and the two TGFB receptors (TGFBR1 and TGFBR2) were highly expressed in supporting cells surrounding OHCs at postnatal days 1–3 and day 23 (Figures S7B–S7J). Together, these data provide strong evidence that the VEGFR inhibitor regorafenib promotes hair cell reprogramming via downregulation of *Tgfb1* expression and inhibition of TGFB signaling.

DISCUSSION

Protection and regeneration of the mammalian cochlear hair cells are essential for hearing restoration; however, efforts to identify the key regulators of these processes has been hampered by the lack of high-throughput *in vitro* models. In this study, we establish and characterize a cochlear organoid platform that achieves ~6,000-fold increase in sample output for high-throughput screening of small molecules promoting hair cell differentiation. The identified VEGFR inhibitor robustly induced hair cell reprogramming in normal and injured cochlear explants, through a NOTCH-independent and a TGFB-dependent mechanism. Our study not only highlights the versatility of the cochlear organoid system as a powerful model for auditory research, but also identifies the VEGFR-MEK-TGFB1 signaling axis as a novel target for hair cell regeneration.

Cochlear progenitor cells derived from sensory epithelia of neonatal mouse can be efficiently expanded and differentiated into hair cells (Lenz et al., 2019; McLean et al., 2017). Our study represents the first high-throughput screening effort using cochlear organoids. The identified FDA-approved small-molecule regorafenib was successfully validated on normal and injured cochlear explants, suggesting that the cochlear organoids are a valid *in vitro* model for hair cell reprogramming studies. Together with a previous report (McLean et al., 2017), we also show that *in vitro* differentiation of hair cells in the organoid recapitulates the embryonic development of cochlear hair cells, including dynamic expression of hair cell markers, regulations of stereocilia and kinocilia, and formation of presynaptic ribbons. Thus, the cochlear organoid may also serve as an excellent model for studying mechanisms and regulators of hair cells during embryonic development. In addition, the cochlear organoids could also be robustly transduced by lentiviruses and gene edited using CRISPR-Cas9 (Lenz et al., 2019). Thus, cochlear organoids may serve as a powerful platform for high-throughput studies involving virus-mediated gene expression or editing.

Nevertheless, the cochlear organoid model used in this study is not without pitfalls. Firstly, continuous propagation and long-term maintenance of the cochlear organoids remains a challenge. Unlike the intestinal organoids, which can be passaged quasi-infinitely without losing stemness (Lee et al., 2018), the current cochlear organoids can only be effectively maintained within two passages despite our optimization efforts. Further optimization of the culture conditions needs to be performed in a systematic manner to achieve long-term propagation of the cochlear organoids. Secondly, the organoids were derived from early postnatal mouse cochlea, whereas dissociated

(B) Regorafenib downregulated *Tgfb1* expression via the MAPK pathway. MAPK (MEK) inhibitor U0126 but not PI3K inhibitor wortmannin abolished the effect of regorafenib on *Tgfb1* expression. Error bars represent mean ± SEM. n = 3 independent experiments with six cochlear explants at each condition. *p < 0.05, **p < 0.01, ***p < 0.001 by one-way ANOVA.

(C and D) Regorafenib treatment downregulated SMAD2 phosphorylation in cochlear explants. Cochlear explants were treated with regorafenib (10 μM) for 12 h. (C) Western blot graphs and (D) densitometric quantification of SMAD2 phosphorylation. Error bars represent mean ± SEM. n = 3 independent experiments with six to seven cochlear explants. *p < 0.05 by Student's t test.

(E) SMAD2 phosphorylation was induced by TGFB1 treatment and inhibited by TGFB type I receptor inhibitor SB431542 (SB). Cochlear explants were treated with TGFB1 (10 ng/mL) and/or SB431542 (10 μM) for 6 h.

(F and G) Inhibition of TGFB signaling by SB431542 promoted hair cell reprogramming in cochlear explants. (F) Hair cell counts and (G) confocal images of cochlear explants treated with SB431542. Error bars represent mean ± SEM. n = 3–12 cochlear explants at each condition. *p < 0.05, **p < 0.01, ***p < 0.001 by one-way ANOVA. Scale bars, 20 μm.

(H and I) Effect of regorafenib in downregulation of SMAD2 phosphorylation was abolished by co-treatment with TGFB1 recombinant protein in cochlear explants. (H) Western blot graphs and (I) densitometric quantification of SMAD2 phosphorylation. Cochlear explants were treated with TGFB1 (10 ng/mL) and/or regorafenib (10 μM) for 12 h. Error bars represent mean ± SD. n = 4 cochlear explants from two independent experiments. *p < 0.05 and **p < 0.01 by one-way ANOVA to vehicle control and ^p < 0.05 between Reg and Reg + TGFB1.

(J and K) TGFB1 recombinant protein abolished the effect of regorafenib on hair cell reprogramming. (J) Confocal images of hair cell markers and (K) hair cell counts of cochlear explants treated with regorafenib (1 μM) alone or together with TGFB1 recombinant protein (0.25, 0.5, or 1 ng/mL). DAPT (10 μM) alone and TGFB1 (1 ng/mL) alone were controls. Scale bars, 20 μm. Error bars represent mean ± SEM. n = 4–10 cochlear explants at each condition. ***p < 0.001 by one-way ANOVA compared with vehicle control (open bar). ^p < 0.05, ^^^p < 0.001 by one-way ANOVA compared with regorafenib alone (red bar).

See also Figures S5 and S7.

cells from adult mouse cochlea showed very limited expansion. Although the LGR5+ supporting cells remain present in the adult cochlea (Shi et al., 2012), the activities of ATOH1, WNT signaling, and NOTCH pathways appear to be reduced compared with neonatal aged samples (Roccio and Edge, 2019). It is likely that additional co-factors are required for successful expansion of adult progenitor cells *in vitro*. Thirdly, cochlear organoids generated from neonatal sensory epithelia were heterogeneous and show variability in the potency and dynamics in hair cell differentiation, suggesting that distinct signaling pathways may be required for induction of hair cell formation from distinct supporting cell subpopulations. Finally, a robust human cochlear organoid model is still lacking. Due to limitations in sample acquisition and ethical concerns, progenitor cells from human cochleae are rarely available (McLean et al., 2017). Instead, inner ear organoids could be obtained by 3D culture and staged induction from human pluripotent stem cells (Koehler et al., 2017). However, only a small proportion of the inner ear organoids contain differentiated hair cells and the induced hair cells from stem cell-derived organoids display vestibular but not cochlear characteristics (Koehler et al., 2017; Liu et al., 2016). Therefore, further optimizations of the human inner ear organoids for robust generation of cochlear hair cells will be a major challenge and a worthy undertaking.

Our finding reveals that VEGF and TGFB crosstalk acts as a repressive signal for hair cell reprogramming. VEGF is widely expressed in cochlea, including cells of the organ of Corti, stria vascularis, spiral ligament, and spiral ganglion (Michel et al., 2001). TGFB1 is expressed in the stria vascularis, supporting cells of the inner hair cells and Deiters cells (Bas et al., 2019). Both FLT1 and KDR are expressed in cochlear supporting cells and spiral ganglion neurons (Michel et al., 2001), suggesting that these cells respond to VEGF signaling. Our data indicate that VEGFR signaling in cochlear supporting cells regulates TGFB1 expression via the MEK pathway, which is consistent with the co-localization of KDR and TGFB1 in these cells (Bas et al., 2019; Michel et al., 2001). As we show that the TGFB receptors TGFBR1 and TGFBR2 are also expressed in these supporting cells, it is likely that TGFB1 acts as an autocrine or paracrine signal to inhibit hair cell trans-differentiation. However, whether the VEGF and TGFB crosstalk plays an important role in hair cell development and supporting cell maintenance *in vivo* remains to be examined in future.

TGFB is a well-known signaling pathway involved in proliferation and differentiation of embryonic and somatic stem cells (Mullen and Wrana, 2017; Yu and Feng, 2019). Inhibition of TGFB signaling is important for non-neural ectoderm induction at early differentiation stages of embryonic stem cell-derived inner ear organoids (Koehler et al., 2013, 2017). In addition, as TGFB regulates cellular quiescence (Hua and Thompson, 2001), TGFB inhibition is required for efficient expansion of the LGR5+ cochlear progenitor cells (McLean et al., 2017). Our data suggest that the TGFB signaling, presumably regulated by VEGFRs in supporting cells, also plays an important inhibitory role for hair cell reprogramming. Consistent with this notion, inhibition of BMP, also acting on the TGFB pathway, promotes hair cell regeneration in the chicken cochlea (Jiang et al., 2018). While our study provides important *in vitro* data for the involvement of VEGFR-MEK-TGFB1 signaling in hair cell fate conversion, the *in vivo* evidence is still lacking. Pharmacological or direct genetic manipulations of TGFB signaling in mammalian cochlea *in vivo* will be important next steps toward better understanding the roles of TGFB in hair cell development and regeneration.

Our results suggest that the VEGFR-MEK-TGFB1 axis promotes hair cell reprograming and maturation in a NOTCH-independent pathway. Intriguingly, we found that inhibition of VEGFR-MEK-TGFB1 but not NOTCH signaling promotes presynaptic ribbon formation in reprogrammed hair cells, suggesting that TGFB signaling may play a unique role in synaptic formation. To date, the interplay between WNT and NOTCH signaling is thought to be instrumental to hair cell fate determination and regeneration, as they appear to converge on key transcription factors, such as SOX2 and ATOH1 (Samarajeewa et al., 2019). As inhibition of VEGFR and NOTCH synergistically promotes hair cell reprogramming, the VEGFR-MEK-TGFB1 signaling axis provides an important additional target for studying hair cell development, maturation, and regeneration in the mammalian cochlea.

EXPERIMENTAL PROCEDURES

Mouse strains

Lgr5-EGFP-IRES-CreER (no. 008875) (Barker et al., 2007), *Plp1-CreER* (no. 005975) (Doerflinger et al., 2003), *Sox2-CreER* (no. 017593) (Arnold et al., 2011), and *Rosa26*-ACTB-*mTmG* (no. 007676) (Muzumdar et al., 2007) were obtained from the Jackson Laboratory. *Rosa26*-CAG-*STOP-Cas9-tdTomato* (*Rosa26-tdTomato*) mice were obtained from GemPharmatech, China. *Pou4f3-EGFP-IRES-CreER* or *Pou4f3(EGFP/+)* knockin mice were generated using the CRISPR-Cas9 genome-editing technology (Du et al., 2020; Zhu et al., 2020). Both male and female mice on a C57BL6 background were used in this study. All animal procedures were approved by the Institutional Animal Care and Use Committee of Model Animal Research Center of Nanjing University, China, with protocol approval no. WGQ01.

Cochlear organoid experiments

Cochlear sensory epithelia were isolated from P3 mice followed by single-cell suspension and 3D culturing. For drug screening studies, cochlear organoids from *Pou4f3(EGFP/+)* mice were differentiated in culture media containing 10 μM of individual small

molecules from the FDA-approved drug library. Details are provided in the supplemental experimental procedures.

Cochlear explant experiments

Cochlear sensory epithelia were isolated from P3 mice and cultured as explants in collagen-coated 35 mm dishes. For lineage-tracing experiments, *Sox2-CreER*:*Rosa26-tdTomato* cochlear explants were cultured in medium containing 4-hydroxytamoxifen. For neomycin-injured experiments, cochlear explants were cultured in medium containing 0.15 M neomycin.

Immunofluorescence

Cochlear organoids or explants were wash three times with PBS, and then fixed at room temperature with 4% paraformaldehyde/PBS for 20 min and then washed three times with PBS. Immunostaining procedures are described in the supplemental experimental procedures. All imaging was carried out using a Zeiss LSM880 confocal microscope (Zeiss, Germany).

Gene expression analyses

Total RNA from cochlear organoids or explants were extracted using RNAiso Plus (TaKara, Japan). Cochlear explants were washed once with PBS and 1 mL RNAiso Plus was added. qRT-PCR and RNA-seq are detailed in the supplemental experimental procedures.

Statistical analysis

Statistical significance was determined by unpaired Student's t test to compare two groups or by one-way ANOVA to compare multiple experimental groups using GraphPad Prism 8.

Data and code availability

The RNA-seq data are available at the GEO database under accession no. GSE139485.

SUPPLEMENTAL INFORMATION

Supplemental information can be found online at https://doi.org/10.1016/j.stemcr.2021.08.010.

AUTHOR CONTRIBUTIONS

G.W. conceived the study. Q.L. and G.W. designed the experiments. Q.L. performed all the organoid culture and cochlear explant works. L.Z. generated the *Pou4f3(EGFP/+)* knockin mouse line. M.-S.Z. provided the FDA-approved small-molecule library. Q.L. and G.W. wrote the manuscript with the help from other authors.

CONFLICTS OF INTEREST

Q.L. and G.W. filed a pending patent application on the use of regorafenib and related chemicals for hair cell regeneration. The other authors do not have competing interests.

ACKNOWLEDGMENTS

We thank Gabriel Corfas (University of Michigan) for critical reading of the manuscript. This work was supported by grants from the National Natural Science Foundation of China (31771153 and 81970888 to G.W., and 31330034 and 31671548 to M.S.Z.) and the Fundamental Research Funds for the Central Universities (0903-1480601101 to G.W.).

Received: June 11, 2021
Revised: August 17, 2021
Accepted: August 17, 2021
Published: September 14, 2021

REFERENCES

Arnold, K., Sarkar, A., Yram, M.A., Polo, J.M., Bronson, R., Sengupta, S., Seandel, M., Geijsen, N., and Hochedlinger, K. (2011). Sox2(+) adult stem and progenitor cells are important for tissue regeneration and survival of mice. Cell Stem Cell *9*, 317–329.

Atkinson, P.J., Dong, Y., Gu, S., Liu, W., Najarro, E.H., Udagawa, T., and Cheng, A.G. (2018). Sox2 haploinsufficiency primes regeneration and Wnt responsiveness in the mouse cochlea. J. Clin. Invest. *128*, 1641–1656.

Barker, N., Tan, S., and Clevers, H. (2013). Lgr proteins in epithelial stem cell biology. Development *140*, 2484–2494.

Barker, N., van Es, J.H., Kuipers, J., Kujala, P., van den Born, M., Cozijnsen, M., Haegebarth, A., Korving, J., Begthel, H., Peters, P.J., and Clevers, H. (2007). Identification of stem cells in small intestine and colon by marker gene Lgr5. Nature *449*, 1003–1007.

Bas, E., Anwar, M.R., and Van De Water, T.R. (2019). TGF beta-1 and WNT signaling pathways collaboration associated with cochlear implantation trauma-induced fibrosis. Anat. Rec. (Hoboken). *303*, 608–618.

Bramhall, N.F., Shi, F., Arnold, K., Hochedlinger, K., and Edge, A.S. (2014). Lgr5-positive supporting cells generate new hair cells in the postnatal cochlea. Stem Cell Reports *2*, 311–322.

Chen, P., Johnson, J.E., Zoghbi, H.Y., and Segil, N. (2002). The role of Math1 in inner ear development: uncoupling the establishment of the sensory primordium from hair cell fate determination. Development *129*, 2495–2505.

Coffin, A.B., Ou, H., Owens, K.N., Santos, F., Simon, J.A., Rubel, E.W., and Raible, D.W. (2010). Chemical screening for hair cell loss and protection in the zebrafish lateral line. Zebrafish *7*, 3–11.

Cross, M.J., Dixelius, J., Matsumoto, T., and Claesson-Welsh, L. (2003). VEGF-receptor signal transduction. Trends Biochem. Sci. *28*, 488–494.

Doerflinger, N.H., Macklin, W.B., and Popko, B. (2003). Inducible site-specific recombination in myelinating cells. Genesis *35*, 63–72.

Du, H., Ye, C., Wu, D., Zang, Y.Y., Zhang, L., Chen, C., He, X.Y., Yang, J.J., Hu, P., Xu, Z., et al. (2020). The cation channel TMEM63B is an osmosensor required for hearing. Cell Rep. *31*, 107596.

Fatehullah, A., Tan, S.H., and Barker, N. (2016). Organoids as an in vitro model of human development and disease. Nat. Cell Biol. *18*, 246–254.

Ferrara, N., Gerber, H.P., and LeCouter, J. (2003). The biology of VEGF and its receptors. Nat. Med. *9*, 669–676.

Fettiplace, R., and Hackney, C.M. (2006). The sensory and motor roles of auditory hair cells. Nat. Rev. Neurosci. *7*, 19–29.

Fuchs, P.A., Glowatzki, E., and Moser, T. (2003). The afferent synapse of cochlear hair cells. Curr. Opin. Neurobiol. *13*, 452–458.

Grothey, A., Cutsem, E.V., Sobrero, A., Siena, S., Falcone, A., Ychou, M., Humblet, Y., Bouché, O., Mineur, L., Barone, C., et al. (2013). Regorafenib monotherapy for previously treated metastatic colorectal cancer (CORRECT): an international, multicentre, randomised, placebo-controlled, phase 3 trial. Lancet *381*, 303–312.

Hua, X., and Thompson, C.B. (2001). Quiescent T cells: actively maintaining inactivity. Nat. Immunol. *2*, 1097–1098.

Jansson, L., Kim, G.S., and Cheng, A.G. (2015). Making sense of Wnt signaling-linking hair cell regeneration to development. Front. Cell Neurosci. *9*, 66.

Jiang, L., Xu, J., Jin, R., Bai, H., Zhang, M., Yang, S., Zhang, X., Zhang, X., Han, Z., and Zeng, S. (2018). Transcriptomic analysis of chicken cochleae after gentamicin damage and the involvement of four signaling pathways (Notch, FGF, Wnt and BMP) in hair cell regeneration. Hearing Res. *361*, 66–79.

Kalinec, G.M., Webster, P., Lim, D.J., and Kalinec, F. (2003). A cochlear cell line as an in vitro system for drug ototoxicity screening. Audiol. Neurootol. *8*, 177–189.

Koehler, K.R., Mikosz, A.M., Molosh, A.I., Patel, D., and Hashino, E. (2013). Generation of inner ear sensory epithelia from pluripotent stem cells in 3D culture. Nature *500*, 217–221.

Koehler, K.R., Nie, J., Longworth-Mills, E., Liu, X.P., Lee, J., Holt, J.R., and Hashino, E. (2017). Generation of inner ear organoids containing functional hair cells from human pluripotent stem cells. Nat. Biotechnol. *35*, 583–589.

Kuo, B.R., Baldwin, E.M., Layman, W.S., Taketo, M.M., and Zuo, J. (2015). In vivo cochlear hair cell generation and survival by coactivation of beta-catenin and Atoh1. J. Neurosci. *35*, 10786–10798.

Lee, S.B., Han, S.H., and Park, S. (2018). Long-term culture of intestinal organoids. Methods Mol. Biol. *1817*, 123–135.

Lenz, D.R., Gunewardene, N., Abdul-Aziz, D.E., Wang, Q., Gibson, T.M., and Edge, A.S.B. (2019). Applications of Lgr5-positive cochlear progenitors (LCPs) to the study of hair cell differentiation. Front. Cell Dev. Biol. *7*, 14.

Liu, H., Chen, L., Giffen, K.P., Stringham, S.T., Li, Y., Judge, P.D., Beisel, K.W., and He, D.Z.Z. (2018a). Cell-specific transcriptome analysis shows that adult pillar and Deiters' cells express genes encoding machinery for specializations of cochlear hair cells. Front. Mol. Neurosci. *11*, 356.

Liu, W., Wang, C., Yu, H., Liu, S., and Yang, J. (2018b). Expression of acetylated tubulin in the postnatal developing mouse cochlea. Eur. J. Histochem. *62*, 2942.

Liu, X.P., Koehler, K.R., Mikosz, A.M., Hashino, E., and Holt, J.R. (2016). Functional development of mechanosensitive hair cells in stem cell-derived organoids parallels native vestibular hair cells. Nat. Commun. *7*, 11508.

McGovern, M.M., Randle, M.R., Cuppini, C.L., Graves, K.A., and Cox, B.C. (2019). Multiple supporting cell subtypes are capable of spontaneous hair cell regeneration in the neonatal mouse cochlea. Development *146*, dev171009.

McLean, W.J., Yin, X., Lu, L., Lenz, D.R., McLean, D., Langer, R., Karp, J.M., and Edge, A.S.B. (2017). Clonal expansion of Lgr5-positive cells from mammalian cochlea and high-purity generation of sensory hair cells. Cell Rep. *18*, 1917–1929.

Mellado Lagarde, M.M., Wan, G., Zhang, L., Gigliello, A.R., McInnis, J.J., Zhang, Y., Bergles, D., Zuo, J., and Corfas, G. (2014). Spontaneous regeneration of cochlear supporting cells after neonatal ablation ensures hearing in the adult mouse. Proc. Natl. Acad. Sci. U S A *111*, 16919–16924.

Michel, O., Hess, A., Bloch, W., Schmidt, A., Stennert, E., and Addicks, K. (2001). Immunohistochemical detection of vascular endothelial growth factor (VEGF) and VEGF receptors Flt-1 and KDR/Flk-1 in the cochlea of Guinea pigs. Hearing Res. *155*, 175–180.

Mizutari, K., Fujioka, M., Hosoya, M., Bramhall, N., Okano, H.J., Okano, H., and Edge, A.S. (2013). Notch inhibition induces cochlear hair cell regeneration and recovery of hearing after acoustic trauma. Neuron *77*, 58–69.

Mullen, A.C., and Wrana, J.L. (2017). TGF-beta family signaling in embryonic and somatic stem-cell renewal and differentiation. Cold Spring Harb. Perspect. Biol. *9*, a022186.

Muzumdar, M.D., Tasic, B., Miyamichi, K., Li, L., and Luo, L. (2007). A global double-fluorescent Cre reporter mouse. Genesis *45*, 593–605.

Olusanya, B.O., Neumann, K.J., and Saunders, J.E. (2014). The global burden of disabling hearing impairment: a call to action. Bull. World Health Organ *92*, 367–373.

Roccio, M., and Edge, A.S.B. (2019). Inner ear organoids: new tools to understand neurosensory cell development, degeneration and regeneration. Development *146*, dev177188.

Rubel, E.W., Furrer, S.A., and Stone, J.S. (2013). A brief history of hair cell regeneration research and speculations on the future. Hearing Res. *297*, 42–51.

Samarajeewa, A., Jacques, B.E., and Dabdoub, A. (2019). Therapeutic potential of Wnt and Notch signaling and epigenetic regulation in mammalian sensory hair cell regeneration. Mol. Ther. *27*, 904–911.

Schaefer, S.A., Higashi, A.Y., Loomis, B., Schrepfer, T., Wan, G., Corfas, G., Dressler, G.R., and Duncan, R.K. (2018). From otic induction to hair cell production: pax2(EGFP) cell line illuminates key stages of development in mouse inner ear organoid model. Stem Cells Dev. *27*, 237–251.

Schmitz, F., Konigstorfer, A., and Sudhof, T.C. (2000). RIBEYE, a component of synaptic ribbons: a protein's journey through evolution provides insight into synaptic ribbon function. Neuron *28*, 857–872.

Shi, F., Kempfle, J.S., and Edge, A.S. (2012). Wnt-responsive Lgr5-expressing stem cells are hair cell progenitors in the cochlea. J. Neurosci. *32*, 9639–9648.

Teitz, T., Fang, J., Goktug, A.N., Bonga, J.D., Diao, S., Hazlitt, R.A., Iconaru, L., Morfouace, M., Currier, D., Zhou, Y., et al. (2018). CDK2 inhibitors as candidate therapeutics for cisplatin- and noise-induced hearing loss. J. Exp. Med. *215*, 1187–1203.

Wagner, E.L., and Shin, J.B. (2019). Mechanisms of hair cell damage and repair. Trends Neurosciences *42*, 414–424.

Wan, G., Corfas, G., and Stone, J.S. (2013). Inner ear supporting cells: rethinking the silent majority. Semin. Cel. Dev. Biol. *24*, 448–459.

Wang, J., and Puel, J.L. (2018). Toward cochlear therapies. Physiol. Rev. *98*, 2477–2522.

Warchol, M.E. (2011). Sensory regeneration in the vertebrate inner ear: differences at the levels of cells and species. Hearing Res. *273*, 72–79.

Wilhelm, S.M., Dumas, J., Adnane, L., Lynch, M., Carter, C.A., Schutz, G., Thierauch, K.H., and Zopf, D. (2011). Regorafenib (BAY 73-4506): a new oral multikinase inhibitor of angiogenic, stromal and oncogenic receptor tyrosine kinases with potent preclinical antitumor activity. Int. J. Cancer *129*, 245–255.

Xiang, M., Maklad, A., Pirvola, U., and Fritzsch, B. (2003). Brn3c null mutant mice show long-term, incomplete retention of some afferent inner ear innervation. BMC Neurosci. *4*, 2.

Yu, Y., and Feng, X.H. (2019). TGF-beta signaling in cell fate control and cancer. Curr. Opin. Cell Biol. *61*, 56–63.

Zhu, G.J., Gong, S., Ma, D.B., Tao, T., He, W.Q., Zhang, L., Wang, F., Qian, X.Y., Zhou, H., Fan, C., et al. (2020). Aldh inhibitor restores auditory function in a mouse model of human deafness. PLoS Genet. *16*, e1009040.